Journal of
Materials Chemistry B

Accepted Manuscript

ROYAL SOCIETY OF CHEMISTRY

www.rsc.org/materialsB

# Cyclodextrins functionalized hollow carbon nanospheres by introducing nanogold for enhanced electrochemical sensing of o-dihydroxybenzene and p-dihydroxybenzene

Gangbing Zhu [a,*], Yinhui Yi [a], Heng Sun [a], Kun Wang [b,*], Zhixiang Han [a], Xiangyang Wu [a,*]

[a] School of the Environment and Safety Engineering, Jiangsu University, Zhenjiang, 212013, P. R.China

[b] School of Chemistry and Chemical Engineering, Jiangsu University, Zhenjiang 212013, P. R. China

## Abstract

In this work, hollow carbon nanospheres (HCNS) were prepared and followed by introducing gold nanoparticles (AuNPs) on HCNS surface, and then functionalized with per-6-thio-β-cyclodextrin (CD) based on the formation of “Au-S” bond, resulting a novel cyclodextrin/carbon-based nanohybrid (CD-AuNPs/HCNS) which possesses the unique properties of HCNS (excellent electrochemical properties and large surface area), CD (high host-guest recognition and water-solubility) and AuNPs (excellent electrocatalytic activity). The obtained CD-AuNPs/HCNS nanohybrids were characterized by scanning electron microscopy, transmission electron microscopy, inductively coupled plasma-atomic emission spectroscopy, Fourier transform infrared spectroscopy and electrochemical methods, et al. Further, the CD-AuNPs/HCNS were applied in simultaneous electrochemical sensing of o-dihydroxybenzene (o-DHB) and p-dihydroxybenzene (p-DHB) (both of o- and p-DHB have similar structures and coexist in environment, and meanwhile they are toxic to humans and difficult to degrade). Under the optimum conditions, the detection limits of o- and p-DHB obtained in this work are 0.01 and 0.02 μM, respectively.

---

* E-mail address: zhgb1030@ujs.edu.cn (G. Zhu); wangkun@ujs.edu.cn (K. Wang); wuxy@ujs.edu.cn (X. Wu).

## Introduction

Two kinds of dihydroxybenzene isomers, o-dihydroxybenzene (o-DHB) and p-dihydroxybenzene (p-DHB) are frequently used as industrial reagents in the production of plastic, tanning, paint, cosmetics, dyes, rubber and pharmaceuticals.[1-3] However, both of o- and p-DHB exist widely in environment as a kind of important environmental pollutants because they are toxic to humans and difficult to degrade. Owing to the similar structures, properties, and coexistence in environmental samples, thus the simultaneous determination of o- and p-DHB is very important. Up to now, many electrochemical sensors have been designed to detect o- and p-DHB.[4] Unfortunately, o- and p-DHB usually can't be distinguished on the conventional electrodes for the overlap of their oxidation-reduction peaks.[5] Recently, some interesting works have been developed to resolve this problem,[4, 6] but highly sensitive simultaneous electrochemical determination for o- and p-DHB is still a great challenge.

On the other hand, considerable attentions have been paid to hollow nanostructures because of their fascinating properties (e.g., low density, high surface-to-volume ratio, shell permeability) and promising applications in a wide range of areas.[7] Among the families experienced impressive advances, hollow carbon nanospheres (HCNS, one kind of carbon-based materials) are interesting owing to the outstanding properties of carbon such as cheap, nontoxic, good chemical stability and electrical conductivity, thus HCNS have been applied widely in catalysis,[8, 9] lithium-ion battery,[10, 11] oxygen-reduction,[12] supercapacitor[13] and water treatment.[14, 15] However, there are only few works on the applications of HCNS in electrochemical sensors. In addition, the unmodified pure HCNS are usually insoluble in water, resulting in the severe restriction of their applications. Therefore, designing or introducing new functional molecules to increase the dispersibility of HCNS and meanwhile introduce new or enhanced functions for electrochemical sensors is highly desirable and technologically important.

Cyclodextrins (CDs) are oligosaccharides composed of six, seven, or eight glucose units (α-, β-, or γ-CD, respectively), which are toroidal in shape with a hydrophobic inner cavity and a hydrophilic exterior.[16-18] These interesting characteristics can enable them as solubilizer to improve the water-solubility of functional materials, and meanwhile can make them bind selectively with a large variety of hydrophobic organic molecules into the cavities of CDs to form stable host-guest inclusion complexes, showing high molecular selectivity and enantioselectivity.[19, 20] Therefore, if HCNS are modified with CDs and then used in electrochemical sensors, it is possible to obtain a new functionalized material which has excellent electrochemical sensor performance for highly sensitive and selective determination of targets.

In fact, many attempts, including noncovalent exohedral interactions and covalent sidewall coupling reactions, have been developed to produce CDs/carbon-based (mainly focused on carbon nanotubes and graphene) nanohybrids for obtaining the synergetic effects of CDs (*e.g.* a hydrophilic external surface and a high supramolecular recognition and enrichment capability) and carbon-based materials (*e.g.* good electrochemical properties and a large surface area). For noncovalent interactions, a high aromatic molecule, such as 1-pyreneacetic acid,[17, 21] 3,4,9,10-perylene tetracarboxylic acid,[22] *p*-phenylenediamine,[23] aniline polypseudorotaxane,[24] tris[4,4-bis(4-pyren-1-ylbutyloxy)bipyridinyl)] iron complex[25] and adamantine,[26] is usually used as a bridge between CDs and carbon-based materials. For covalent reactions, chemical oxygen groups are needed on the surface of carbon-based materials to react with CDs by esterification reaction,[27] sulfonylation reaction[28] and et al.[29, 30] Although the carbon-based materials could be successfully functionalized with CDs by these methods, there are many disadvantages: (i) complex synthesis procedures, (ii) reduction of effective surface area, (iii) loss of their electronic conductivity and corrosion resistance, (iv) structural damage of the carbon nanomaterials. These are not beneficial for enhancing the electrochemical sensor performance of CDs/carbon-based nanohybrids.

It was reported that dihydroxybenzene isomers could bind to the cavity of β-CD to form a stable host guest inclusion and that the ability to associate with β-CD varies for different isomers,[18] thus indicating that β-CD could be used to selective detection of o- and p-DHB. Based on the above facts, HCNS were prepared herein by polymerization and carbonization of dopamine hydrochloride (DA) (Scheme S1). Then, by decorating gold nanoparticles (AuNPs) on HCNS surface to form AuNPs/HCNS hybrids, followed by functionalizing AuNPs/HCNS with per-6-thio-β-cyclodextrin (CD, Figure S1), a novel nanohybrid (denoted as CD-AuNPs/HCNS) was obtained. The CD-AuNPs/HCNS could show the synergetic effects from HCNS, CD and AuNPs. Importantly, compared to the previous methods for preparing CDs/carbon-based nanohybrids, the method presented in this paper is simple, convenient and low-cost coupling with the advantages as follow: the effective surface area, electronic conductivity, corrosion resistance, and structural of carbon-based nanohybrids aren't reduced or damaged obviously due to the absence of high aromatic molecules and chemical oxygen groups. The CD-AuNPs/HCNS modified glassy carbon (GC) (CD-AuNPs/HCNS/GC) electrode was applied for the simultaneous electrochemical determination of o- and p-DHB with cyclic voltammetry (CV) and differential pulse voltammetry (DPV), the results show that the electrochemical performance of o- and p-DHB at the CD-AuNPs/HCNS/GC electrode is improved obviously and low detection limits for o-DHB and p-DHB are achieved. The procedures for preparing CD-AuNPs/HCNS and constructing electrochemical sensor for o- and p-DHB are shown in Scheme 1.

## Experimental Section

### Reagents and apparatus

o-DHB, p-DHB, DA and $SiO_2$ particles were purchased from Alfa Aesar (USA). CD was purchased from Shandong Binzhou Zhiyuan Bio-Technology Co. Ltd., China. All other chemicals were of analytical grade and used directly without further purification. The supporting electrolyte was 0.1 M phosphate buffer solution (PBS) prepared with $Na_2HPO_4$ and $NaH_2PO_4$. Aqueous solutions used throughout were prepared with ultra pure water (>18 MΩ cm) obtained from a Millipore system.

All electrochemical measurements were performed on a CHI 660E Electrochemical Workstation (Chenhua Instrument Company of Shanghai, China). A conventional three-electrode cell was used with a GC electrode (GC, with a diameter of 3 mm) as the working electrode, a platinum wire as the counter electrode and an Ag/AgCl electrode (saturated KCl) electrode as the reference electrode. Except the specific statement, the electrochemical measurements were carried out in 0.1 M PBS (pH 7.0) at room temperature (25 ± 2 °C). All the potentials in this paper were referred to Ag/AgCl electrode (saturated KCl).

### Synthesis of HCNS, AuNPs/HCNS and CD-AuNPs/HCNS

**HCNS**: The synthesis of HCNS was prepared according to the previous report.[9, 14] In briefly, $SiO_2$ particles (100.0 mg) were washed thoroughly with tris(hydroxymethyl)aminomethane (TRIS) buffer (50.0 mM; pH = 8.5) and mixed with 40.0 mL TRIS buffer containing DA (80.0 mg) for 24 h by vigorous stirring, the silica@polydopamine ($SiO_2$@PDA) nanocomposites were obtained by centrifugation and drying in vacuum at 60 °C overnight. For preparing HCNS, the $SiO_2$@PDA nanocomposites were carbonized under $N_2$ atmosphere at 800 °C for 2 h with a heating rate of 5 °C $min^{-1}$. After washing in 2.0 M HF + 8.0 M $NH_4F$ solution for 8 h, the template ($SiO_2$) was removed and HCNS were obtained. Finally, the HCNS were washed and dried.

**AuNPs/HCNS**: In ice-water bath, HCNS (10.0 mg) were dispersed in water (10.0 mL) + ethanol (10.0 mL) for 30 min by sonication, and then hydrogen tetrachloroaurate (III) trihydrate and sodium borohydride solutions were added dropwise. After centrifuging and washing thoroughly with ultra pure water, AuNPs/HCNS were obtained successfully.

**CD-AuNPs/HCNS**: Under sonication, 5.0 mL CD solution (1.0 mg $mL^{-1}$) was mixed with 5.0 mL AuNPs/HCNS suspension (1.0 mg $mL^{-1}$) for 24 h in the dark, followed by centrifugation, washing and drying, the CD-AuNPs/HCNS were obtained finally.

### Construction of electrochemical sensor for highly sensitive simultaneous determination of o- and p-DHB

The GC electrode was polished carefully to a mirror like plane with 0.5 and 0.05 μm alumina powder and rinsed with ultra-pure water, followed by sonication in acetone and ultra-pure water, respectively. Then, the electrode was allowed to dry under $N_2$ gas. The CD-AuNPs/HCNS/GC electrode was obtained by casting 10.0 μL CD-AuNPs/HCNS suspension (0.5 mg $mL^{-1}$) on the surface of the GC electrode and dried with an infrared lamp. For comparison, HCNS/GC and AuNPs/HCNS/GC electrodes were prepared via a similar procedure.

The simultaneous determination of o- and p-DHB was carried out in 0.1 M PBS and consisted of two consecutive steps: (1) pre-concentration of target molecules from the solution to the modified electrodes under stirring with a definite accumulation time; and (2) electrochemical measurements by CV and DPV.

## Results and Discussion

### Characterization of CD-AuNPs/HCNS and related materials

Figure 1 shows the scanning electron microscopy (SEM) images of $SiO_2$ particles (Figure 1A), $SiO_2$@PDA (Figure 1B) and HCNS (Figure 1C). It's noted that the diameter of $SiO_2$ particles is ~360 nm and the particles surface is very smooth. For $SiO_2$@PDA nanocomposite, the diameter is ~390 nm, suggesting that the shell thickness of PDA is ~30 nm. Following the carbonization of $SiO_2$@PDA and removal of $SiO_2$, the HCNS were obtained successfully. The morphology of AuNPs/HCNS was further characterized by transmission electron microscopy (TEM). As shown in Figure 2, it is noted that AuNPs were dispersed uniformly on the surface of HCNS and the particle size of AuNPs is distributed mainly between 2.0 and 7.0 nm with an average diameter of 4.0 nm (calculated statistically through measuring 200 AuNPs diameter). The content of AuNPs was evaluated to be 6.2 wt% by inductively coupled plasma-atomic emission spectroscopy.

The functionalization of AuNPs/HCNS with CD was investigated by Fourier transform infrared spectroscopy (FT-IR, Figure 3A). It is noted from curve a that CD-AuNPs/HCNS exhibit typical CD absorption features of the ring vibrations at 578, 757, and 951 $cm^{-1}$, the coupled C-O/C-C stretching/O-H bending vibrations at 1025 and 1063 $cm^{-1}$, the coupled C-O-C stretching/O-H bending vibrations at 1146 $cm^{-1}$, -SH stretching vibrations at 2512 $cm^{-1}$, $CH_2$ stretching vibrations at 2910 $cm^{-1}$, and O-H stretching vibrations at 3421 $cm^{-1}$. In addition, the photo images of AuNPs/HCNS and CD-AuNPs/HCNS dispersing in water were evaluated (Figure 3B). After sonicating for 30 min, the

AuNPs/HCNS still couldn't be dispersed and some black precipitates are observed. However, for the CD-AuNPs/HCNS, it was dissolved well in water due to the good water-solubility of CD. These suggest that the AuNPs/HCNS were functionalized successfully with CD.

Electrochemical impedance analysis (EIS) was further used to investigate the electron transfer behavior of CD-AuNPs/HCNS. Figure 4 shows the EIS results of bare GC (Figure 4a), AuNPs/HCNS/GC (Figure 4b) and CD-AuNPs/HCNS/GC (Figure 4c) electrodes recorded in 5.0 mM $Fe(CN)_6^{3-/4-}$ and 0.1M KCl aqueous solution. It is noted that the fitted charge transfer resistance ($R_{ct}$) value of the AuNPs/HCNS/GC electrode is much lower than that of the bare GC electrode, suggesting that the AuNPs/HCNS has high conductivity. For the CD-AuNPs/HCNS/GC electrode, the slight increase of $R_{ct}$ value is resulted from the poor electronic conductivity of CD, and the electron conductivity of the CD-AuNPs/HCNS (2.2 S $cm^{-1}$) measured via the four-point method is lower than that of AuNPs/HCNS (2.9 S $cm^{-1}$), implying that the CD was functionalized successfully on AuNPs/HCNS.

## Electrochemical behaviors of o-DHB and p-DHB

The electrochemical redox behaviors of 10.00 μM o-DHB and 10.00 μM p-DHB at the bare GC, HCNS/GC, AuNPs/HCNS/GC and CD-AuNPs/HCNS/GC electrodes were investigated in 0.1 M PBS by CV (Figure 5). From Figure 5a, it is noted that a broad oxidation peak was observed at ~0.224 V on the GC electrode due to the overlap of the oxidation peaks of o- and p-DHB, and two weak reduction peaks were observed at ~0.152 V and 0.039 V corresponding to the reduction of the oxidation products of o- and p-DHB, respectively. On the HCNS/GC electrode, both of o- and p-DHB exhibit obvious redox peak currents, and the peak separation is up to 0.110 V (oxidation peaks at ~0.210 V for o-DHB and 0.100 V for p-DHB). In addition, two well-defined reduction peaks were observed. The redox currents of o- and p-DHB at the HCNS/GC electrode are much higher than those at the GC electrode. For the values of peak currents on the AuNPs/HCNS/GC electrode, they increase further comparing to the HCNS/GC and GC electrodes. These indicate that both of HCNS and AuNPs have excellent electrocatalytic properties towards o- and p-DHB. After AuNPs/HCNS functionalized with CD, the peak currents of o- and p-DHB at the CD-AuNPs/HCNS/GC electrode were enhanced remarkably and outperform all of the other modified electrodes because of the synergistic effects from HCNS (excellent electrochemical properties and large surface area), CD (high host-guest recognition and water-solubility) and AuNPs (excellent electrocatalytic activity). Specifically, CD could not only increase the dispersibility of HCNS and enhanced the utilization of HCNS-based composites, but also increase the accumulation amount of analytes on the surface of the modified electrodes, thus resulting the sensitivity of CD-AuNPs/HCNS/GC electrode is better than that of AuNPs/HCNS/GC electrode. These suggest that the CD-AuNPs/HCNS nanohybrids have excellent electrochemical sensor performance toward dihydroxybenzene isomers. The reaction mechanisms of o- and p-DHB on the modified electrodes are shown in Scheme 2.

### Optimization of the conditions for the simultaneous electrochemical determination of o-DHB and p-DHB

As a highly sensitive electrochemical method, the DPV has much higher current sensitivity and better resolution compared to CV. So the condition optimization and simultaneous electrochemical detection of o- and p-DHB using CD-AuNPs/HCNS/GC electrode were investigated by DPV.

All of the effects of pH value of PBS, amount of CD-AuNPs/HCNS and accumulation time on the oxidation peak current responses of o- and p-DHB were evaluated by measuring DPV responses of 1.00 μM o-DHB and 1.00 μM p-DHB (Figure 6). It is noted that the peak currents of both of o- and p-DHB increase gradually over the pH range from 5.5 to 7.0, while the pH value exceeded 7.0, the oxidation current decreased rapidly. Therefore, PBS with the pH value of 7.0 was chosen as the supporting electrolyte.

From Figure 6B, it shows that the oxidation peak currents of o- and p-DHB increase with the increase of the amount of CD-AuNPs/HCNS, reaching a maximum at 10.0 μL, and when the amount of CD-AuNPs/HCNS increases further, the peak currents decrease obviously. Therefore, this optimum amount (10.0 μL) was used throughout in this study unless specified otherwise.

Undoubtedly, the sensitivity of the proposed method is affected by the accumulation time. From Figure 6C, it's noted that the oxidation peak currents of o- and p-DHB increase with the increase of the accumulation time and the maximum are observed at 120 s, thus this time is selected as the optimum accumulation time in this work.

### Simultaneous determination of o-DHB and p-DHB

Under the optimum conditions, the CD-AuNPs/HCNS/GC electrode was used to simultaneously detect o- and p-DHB with DPV. In diplex mixture of o- and p-DHB, the concentration of one species changed, and the other remained constant. The DPV responses for different concentrations of o- and p-DHB are shown in Figure 7. From Figure 7A, it is found that the oxidation peak currents of o-DHB increase linearly with the increase of o-DHB concentration from 0.05 to 6.00 μM and the corresponding linear function is $I_p$ (μA)= 0.575 + 1.413 $C$ (μM) ($R^2 = 0.9974$). Similarly, the oxidation peak currents of p-DHB increase with the increase of p-DHB concentration (Figure 7B), and the linear range is 0.05-6.00 μM with the linear function of $I_p$ (μA) = 0.1773 + 1.0561 $C$ (μM) ($R^2 = 0.9933$). The detection limits for o- and p-DHB are 0.01 and 0.02 μM, respectively, which are much lower than those obtained by the electrochemical methods reported previously (Table 1). These results suggest that the proposed method in this work is promising for highly sensitive simultaneous determination of o- and p-DHB.

### Reproducibility, stability and anti-interferent ability of CD-AuNPs/HCNS/GC electrode

The reproducibility and stability of the CD-AuNPs/HCNS/GC electrode were evaluated in 0.1 M PBS containing 1.00 μM o-DHB and 1.00 μM p-DHB. The results reveal that the modified electrode possesses a satisfying reproducibility with a relative standard deviation (RSD) of 4.87 % for 12 parallel measurements with different electrodes. On the other hand, after the modified electrode was stored for 28 days at room temperature, a small current decrease (5.60%) was observed, and this value is 9.75% for 60 days. these reveal that the proposed electrode has good storage stability.

Possible interference during the simultaneous detection of o- and p-DHB at CD-AuNPs/HCNS/GC electrode was also investigated by the addition of various ions and organic pollutants to 0.1 M PBS in the presence of 1.00 μM o-DHB and 1.00 μM p-DHB. The results suggest that no interference was observed for the following inorganic ions: $K^+$, $Na^+$, $Mg^{2+}$, $Al^{3+}$, $Ca^{2+}$, $Zn^{2+}$, $Cl^-$, $SO_4^{2-}$, $NO_3^-$ (50 equiv); similarly, no interference was observed for methanol, ethanol, fenpropathrin, pentachlorophenol, anthracene-9-carbonxylic acid (10 equiv). Especially, in the presence of resorcinol (RC, another dihydroxybenzene isomer), a new oxidation peak of RC was observed at 0.580 V (Figure 8) and the RC didn’t interfere the simultaneous detection of o- and p-DHB, indicating that the proposed modified electrode could be applied in selective simultaneous electrochemical determination for the three kinds of dihydroxybenzene isomers (o-DHB, p-DHB and RC). The above results also demonstrate that the CD-AuNPs/HCNS/GC electrode is suitable for routine simultaneous analysis of o- and p-DHB in practical samples.

### Determination of o-DHB and p-DHB in real water samples

To further explore practical applications, the developed CD-AuNPs/HCNS/GC electrode was used to detect o- and p-DHB in real water samples, which were collected from Changjiang River (Zhenjiang). Certain amounts of o- and p-DHB were spiked in the water samples. After dilution with 0.1 M PBS, the concentrations of o- and p-DHB in each sample were determined by the standard addition method and meanwhile analyzed by high-performance liquid chromatography (HPLC) to testify the accuracy of this method. T-test was performed to compare the values of o- and p-DHB obtained from the proposed method and HPLC (Table 2). It shows that there is no statistically significant differences between the results of analytes obtained with these two methods. Furthermore, it is noted that the quantitative recoveries of 94.9-108.0% are obtained by the electrochemical method. These reveal that the developed method is satisfactory.

## Conclusions

In summary, by introducing AuNPs, HCNS were functionalized successfully with CD based on the formation of “Au-S” bond, resulting a novel CD-AuNPs/HCNS nanohybrid, which possess the synergistic effects from HCNS, CD and AuNPs. For the simultaneous analysis of dihydroxybenzene isomers, the CD-AuNPs/HCNS/GC electrode has a linear response range of 0.05-6.00 μM for both of o- and p-DHB. Comparing with the electrochemical methods for detecting o- and p-DHB reported previously, the method presented in this paper has much lower detection limits (0.01 and 0.02 μM for o- and p-DHB, respectively). Furthermore, the CD-AuNPs/HCNS/GC electrode has high selectivity, good reproducibility and stability. It is believed that this work is very significant to bring a new avenue for the preparation of CDs-functionalized carbon-based materials. Meanwhile, we believe that CD-AuNPs/HCNS hybrids have promising applications in electrochemical sensing and other fields in chiral separation, drug delivery, catalysis and so on.

## Acknowledgements

This work was supported by the National Natural Science Foundation of China (Nos. 21405062, 21175061 and 21375050), the China Postdoctoral Science Foundation (2014M551507), the Scientific Research Foundation for the Talents in Jiangsu University (13JDG091), and Jiangsu Planned Projects for Postdoctoral Research Funds (2014).

## References

1 H.-F. Wang, Y.-Y. Wu and X.-P. Yan, *Anal. Chem.*, 2013, **85**, 1920-1925.

2 V. Vyskočil and J. Barek, *Crit. Rev. Anal. Chem.*, 2009, **39**, 173-188.

3 P. S. d. Silva, B. C. Gasparini, H. A. Magosso and A. Spinelli, *J. Hazard. Mater.*, 2014, **273**, 70-77.

4 Q. Zhang, Y. Qu, X. Zhang, J. Zhou and H. Wang, *Biosens. Bioelectron.*, 2011, **26**, 4362-4367.

5 X. Zhou, Z. He, Q. Lian, Z. Li, H. Jiang and X. Lu, *Sens. Actuators B*, 2014, **193**, 198-204.

6 X. Feng, W. Gao, S. Zhou, H. Shi, H. Huang and W. Song, *Anal. Chim.Acta*, 2013, **805**, 36-44.

7 S. Feng, W. Li, Q. Shi, Y. Li, J. Chen, Y. Ling, A. M. Asiri and D. Zhao, *Chem. Commun.*, 2014, **50**, 329-331.

8 D.-G. Lee, S. M. Kim, H. Jeong, J. Kim and I. S. Lee, *ACS nano*, 2014, **8**, 4510-4521.

9 R. Liu, S. M. Mahurin, C. Li, R. R. Unocic, J. C. Idrobo, H. Gao, S. J. Pennycook and S. Dai, *Angew. Chem. Int. Ed.*, 2011, **50**, 6799-6802.

10 J. Liu, W. Liu, K. Chen, S. Ji, Y. Zhou, Y. Wan, D. Xue, P. Hodgson and Y. Li, *Chem. Eur. J.*, 2013, **19**, 9811-9816.

11 N. Jayaprakash, J. Shen, S. S. Moganty, A. Corona and L. A. Archer, *Angew. Chem.*, 2011, **123**, 6026-6030.

12 Z. L. Schaefer, M. L. Gross, M. A. Hickner and R. E. Schaak, *Angew. Chem.*, 2010, **122**, 7199-7202.

13 X. Fang, J. Zang, X. Wang, M.-S. Zheng and N. Zheng, *J.Mater. Chem. A*, 2014, **2**, 6191-6197.

14 Y. Liu, K. Ai and L. Lu, *Chem. Rev.*, 2014, **114**, 5057-5115.

15 G. Cheng, M.-D. Zhou and S.-Y. Zheng, *ACS Appl. Mater. Interfaces*, 2014, **6**, 12719-12728.

16 A. Harada, Y. Takashima and M. Nakahata, *Acc. Chem. Res.*, 2014, **47**, 2128-2140.

17 Y. Wei, L.-T. Kong, R. Yang, L. Wang, J.-H. Liu and X.-J. Huang, *Chem. Commun.*, 2011, **47**, 5340-5342.

18 X. Chen, S. G. Parker, G. Zou, W. Su and Q. Zhang, *ACS nano*, 2010, **4**, 6387-6394.

19 Á. Martínez, C. O. Mellet and J. M. G. Fernández, *Chem. Soc.Rev.*, 2013, **42**, 4746-4773.

20 G. Zhu, L. Wu, X. Zhang, W. Liu, X. Zhang and J. Chen, *Chem. Eur. J.*, 2013, **19**, 6368-6373.

21 Y.-L. Zhao, L. Hu, J. F. Stoddart and G. Grüner, *Adv. Mater.*, 2008, **20**, 1910-1915.

22 G. Zhu, X. Zhang, P. Gai, X. Zhang and J. Chen, *Nanoscale*, 2012, **4**, 5703-5709.

23 L. Kong, J. Wang, F. Meng, X. Chen, Z. Jin, M. Li, J. Liu and X.-J. Huang, *J.Mater. Chem.*, 2011, **21**, 11109-11115.

24 J. Shi, Y. Chen, Q. Wang and Y. Liu, *Adv. Mater.*, 2010, **22**, 2575-2578.

25 A. Le Goff, K. Gorgy, M. Holzinger, R. Haddad, M. Zimmerman and S. Cosnier, *Chem. Eur. J.*, 2011, **17**, 10216-10221.

26 M. Holzinger, L. Bouffier, R. Villalonga and S. Cosnier, *Biosens. Bioelectron.*, 2009, **24**, 1128-1134.

27 C. Xu, J. Wang, L. Wan, J. Lin and X. Wang, *J.Mater. Chem.*, 2011, **21**, 10463-10471.

28 Y. Gao, Y. Cao, D. Yang, X. Luo, Y. Tang and H. Li, *J. Hazard. Mater.*, 2012, **199**, 111-118.

29 P. Chen, H.-W. Liang, X.-H. Lv, H.-Z. Zhu, H.-B. Yao and S.-H. Yu, *ACS nano*, 2011, **5**, 5928-5935.

30 Y. Guo, S. Guo, J. Ren, Y. Zhai, S. Dong and E. Wang, *ACS nano*, 2010, **4**, 5512-5512.

31 T. C. Canevari, L. T. Arenas, R. Landers, R. Custodio and Y. Gushikem, *Analyst*, 2013, **138**, 315-324.

32 P. Wang, Y. Ni and S. Kokot, *Analyst*, 2013, **138**, 1141-1148.

33 L. Chen, Y. Tang, K. Wang, C. Liu and S. Luo, *Electrochem. Commun.*, 2011, **13**, 133-137.

34 X. Cao, X. Cai, Q. Feng, S. Jia and N. Wang, *Anal. Chim.Acta*, 2012, **752**, 101-105.

35 S.-J. Li, C. Qian, K. Wang, B.-Y. Hua, F.-B. Wang, Z.-H. Sheng and X.-H. Xia, *Sens. Actuators B*, 2012, **174**, 441-448.

36 F. Hu, S. Chen, C. Wang, R. Yuan, D. Yuan and C. Wang, *Anal. Chim.Acta*, 2012, **724**, 40-46.

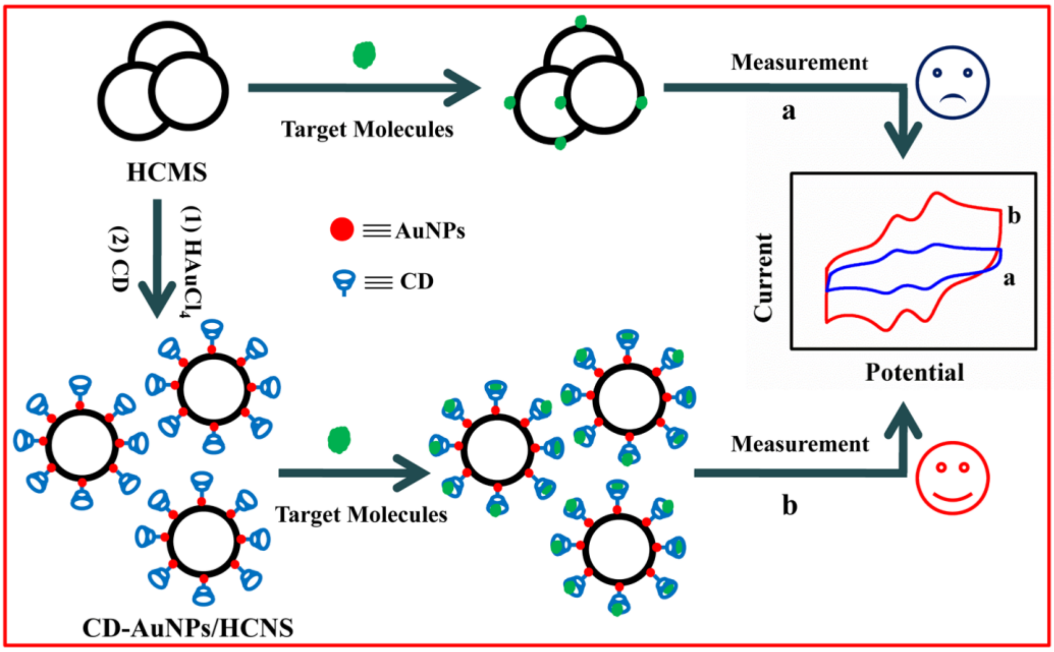

**Scheme 1**. The procedures of preparing CD-AuNPs/HCNS and sensing o- and p-DHB by electrochemical method.

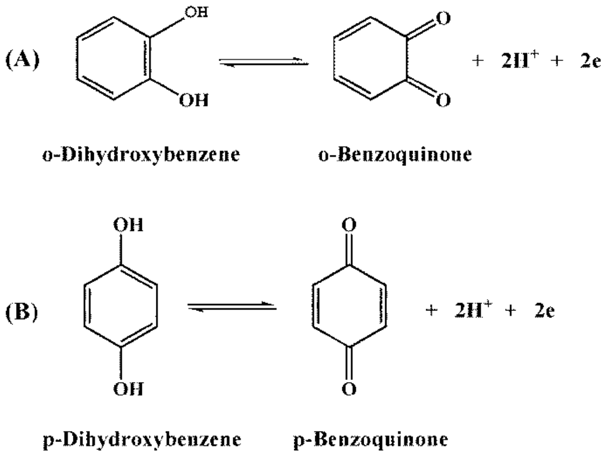

**Scheme 2**. The mechanisms of the electrochemical oxidations of o-DHB (A) and p-DHB (B).

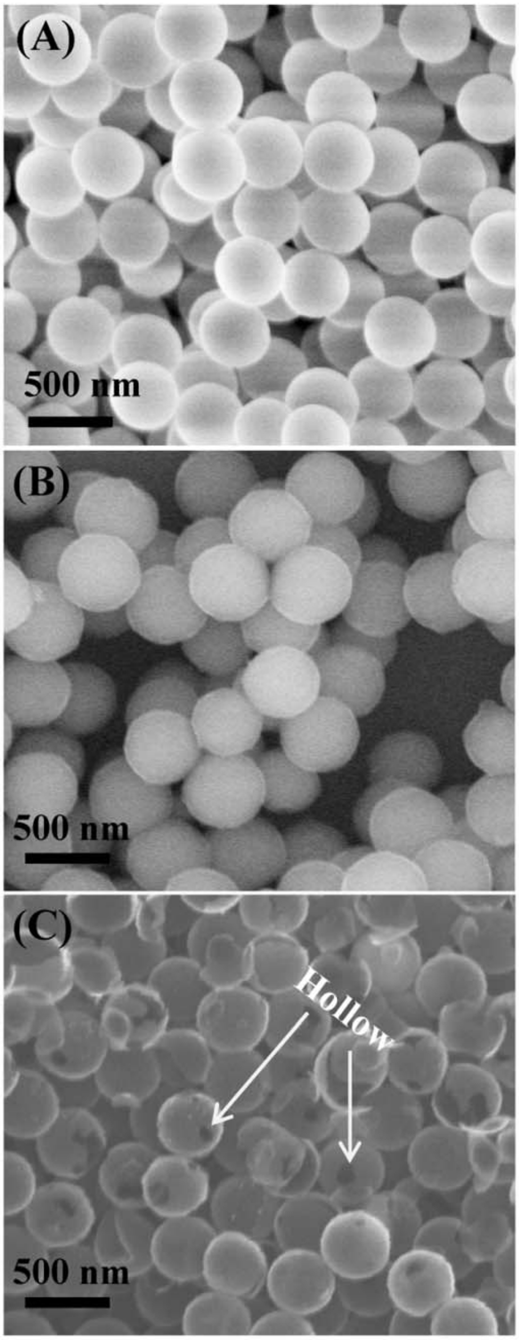

**Figure 1**. SEM images of SiO2 (A), SiO2@PDA (B) and HCNS (C).

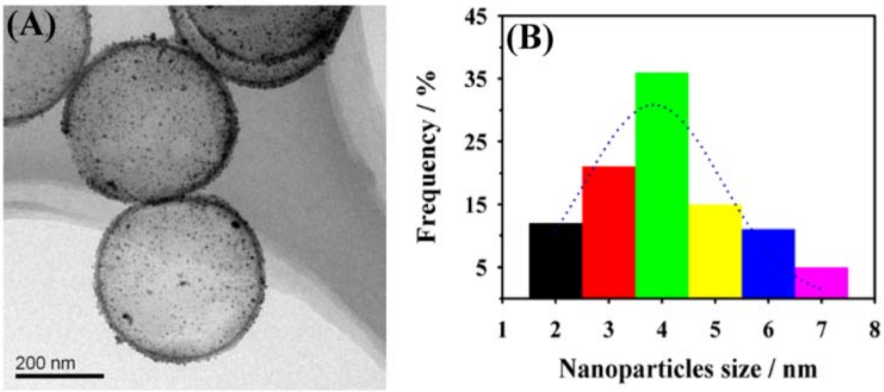

**Figure 2**. (A) TEM image of AuNPs/HCNS and (B) the particle size distribution of AuNPs.

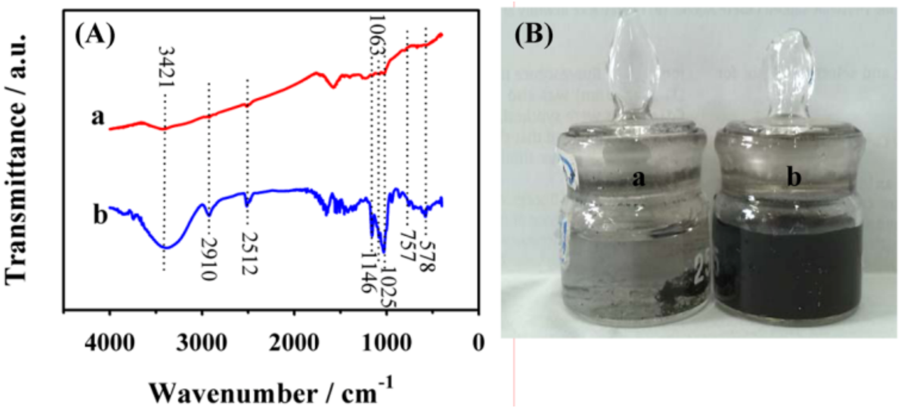

**Figure 3**. (A) The FT-IR spectra of CD-AuNPs/HCNS (a) and CD (b); (B) Photographs of AuNPs/HCNS (a) and CD-AuNPs/HCNS (b) in water.

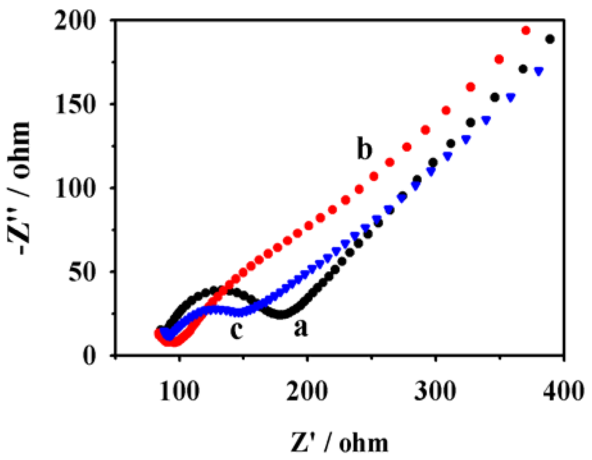

**Figure 4**. EIS plots of the bare GC (a), AuNPs/HCNS/GC (b) and CD-AuNPs/HCNS/GC (c) electrodes in 5.0 mM $Fe(CN)_6^{3-/4-}$ + 0.1 M KCl aqueous solution.

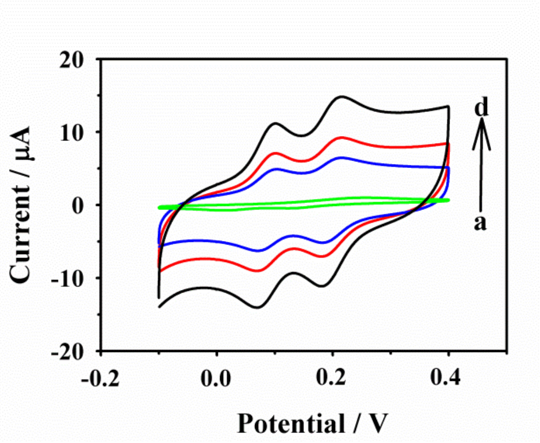

**Figure 5**. Voltammetric responses of 10.00 µM o-DHB and 10.00 µM p-DHB at the bare GC (a), HCNS/GC (b), AuNPs/HCNS/GC (c) and CD-AuNPs/HCNS/GC electrodes (d) in 0.1M PBS.

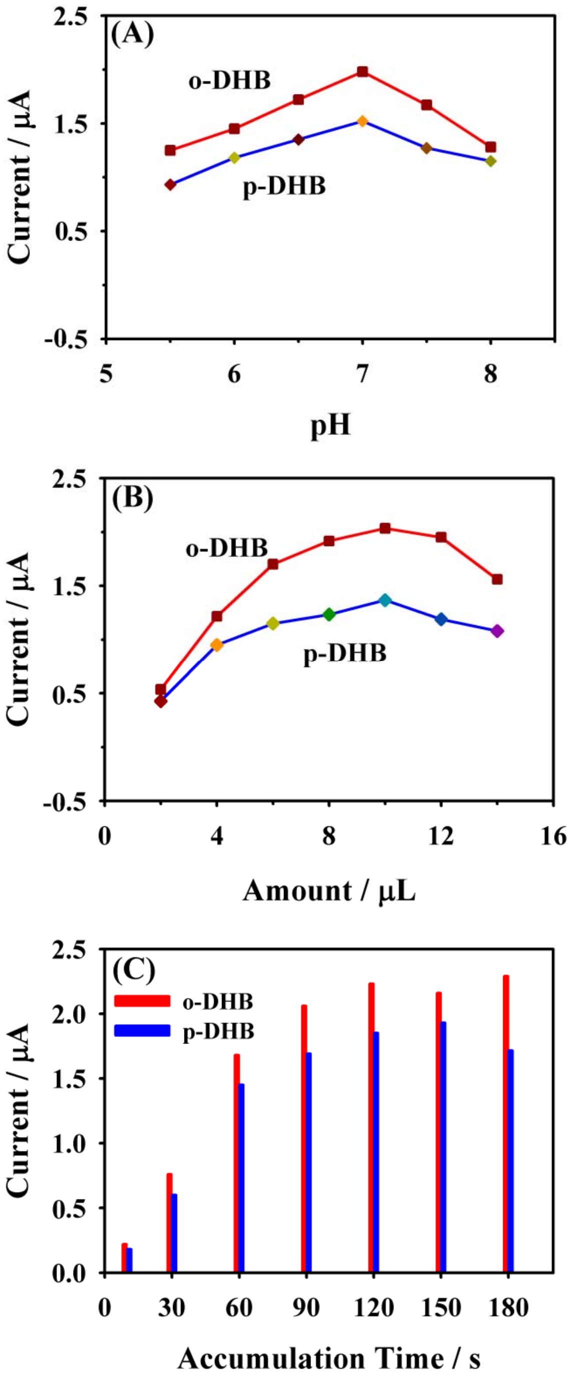

**Figure 6**. The effect of the pH value of the PBS (A), the amount of CD-AuNPs/HCNS (B) and accumulation time (C) on the DPV peak currents of 1.00 μM o-DHB and 1.00 μM p-DHB at the CD-AuNPs/HCNS/GC electrode in 0.1 M PBS.

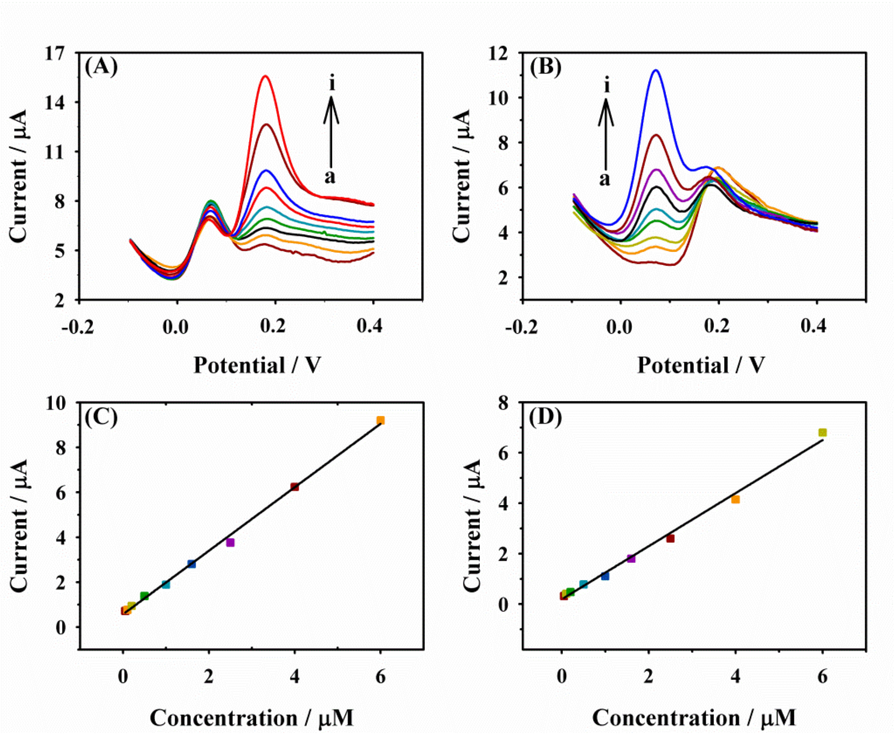

**Figure 7**. DPV responses at the CD-AuNPs/HCNS/GC electrode in 0.1 M PBS (pH 7.0) of samples containing (A) 2.50 µM p-DHB and different concentrations of o-DHB (from a to i: 0.05, 0.10, 0.20, 0.50, 1.00, 1.60, 2.50, 4.00 and 6.00 µM) and (B) 2.50 µM o-DHB and different concentrations of p-DHB (from a to i: 0.05, 0.10, 0.20, 0.50, 1.00, 1.60, 2.50, 4.00 and 6.00 µM). The calibration curves for o-DHB (C) and p-DHB (D) detection.

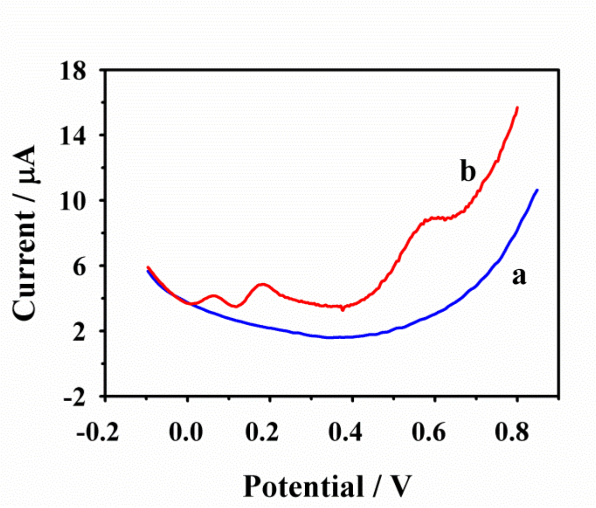

**Figure 8**. DPV responses of the CD-AuNPs/HCNS/GC electrode in 0.1 M PBS without (a) and with (b) o-DHB, p-DHB and RC.

**Table 1**. Comparison of different modified GC electrodes for the determination of o- and p-DHB.

| Electrode | Detection limit (μM) | | Linear range (μM) | | Reference |
|---|---|---|---|---|---|
| | o-DHB | p-DHB | o-DHB | p-DHB | |
| 2,3-Dihydroxybiphenyl 1,2-dioxygenase | 0.428 | | 2.0-800.0 | | 4 |
| Graphene-graphene oxide | 0.2 | 0.16 | 0.5-300.0 | 0.5-300.0 | 5 |
| Polymeric ionic liquid-multiwalled carbon nanotube | 0.17 | 0.40 | 1.0-40.0 | 1.0-50.0 | 6 |
| SiCNb | 0.8 | 1.6 | 39.8-980.0 | 39.8-980.0 | 31 |
| DsDNA/polydiphenylamine-4-sulfonic acid | 0.648 | | 0.75-8.25 | | 32 |
| Reduced graphene oxide | 0.1 | 0.2 | 1.0-200.0 | 6.0-200.0 | 33 |
| CdSe | 0.06 | 0.011 | 0.2-300.0 | 0.6-1500.0 | 34 |
| Thermally reduced graphene oxide | 0.8 | 0.75 | 1.0-500.0 | 1.0-500.0 | 35 |
| Educed graphene oxide-multiwall carbon nanotubes | 1.8 | 2.6 | 5.5-540.0 | 8.0-391.0 | 36 |
| CD-AuNPs/HCNS | 0.01 | 0.02 | 0.05-6.00 | 0.05-6.00 | This work |

**Table 2**. The determination of o- and p-DHB in water samples.

| Water sample | Added (μM) | | Found Mean±SD (μM) | | Recovery Mean±SD (%) | | By HPLC (μM) | | *T*-test [a] | |
|---|---|---|---|---|---|---|---|---|---|---|
| | o-DHB | p-DHB | o-DHB | p-DHB | o-DHB | p-DHB | o-DHB | p-DHB | o-DHB | p-DHB |
| a | 1.00 | 1.00 | 1.08±0.030 | 1.03±0.030 | 108.0±0.030 | 103.0±0.030 | 1.01 | 1.03 | 3.27 | 0.00 |
| b | 2.00 | 2.00 | 2.11±0.050 | 1.96±0.050 | 105.5±0.025 | 98.0±0.025 | 2.08 | 1.97 | 0.84 | -0.28 |
| c | 4.50 | 4.50 | 4.39±0.120 | 4.27±0.170 | 97.6±0.028 | 94.9±0.038 | 4.39 | 4.25 | 0.00 | 0.17 |

[a] *T*-test = ($\bar{x}$ - $\mu_0$) / ($s$ / $\sqrt{n}$ ) , $\bar{x}$ is the average concentration measured by the proposed method in this paper; $\mu_0$ is the concentration measured by HPLC; *n* is the degree of freedom and the confidence level is 95%; $t^{2}_{0.05}$=4.30.

## Table of contents entry

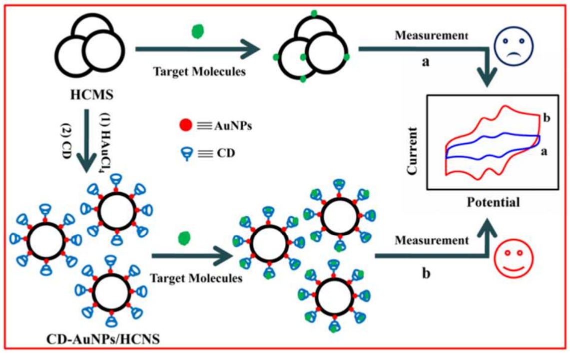

Cyclodextrin-gold nanoparticles/hollow carbon nanospheres nanohybrid was prepared and applied for simultaneous electrochemical sensor of o- and p-dihydroxybenzene, and the obtained nanohybrid shows good analytical performance.